
	Observing Modes and Time Estimation	Ref.: Issue: Date: Page:	BBOP-DAP-RP-0002 0.5 23/06/2020 1/28
---	-------------------------------------	---	---

Title:	B-BOP Observing Modes and Time Estimation		
Date:	23 rd June, 2020	Issue:	0.5
Reference:	BBOP-DAP-RP-0002		
Custodian:			

Authors:	Position:	Date:	Signature:
M. Sauvage	Principal Investigator	23/06/2020	
Contributors:			
D. Dubreuil	Optical Engineer		
J. Delabrouille	Calibration and Observing modes		
Approved by:			
Authorised by:			

The presented document is Proprietary information of the B-BOP Consortium. This document shall be used and disclosed by the receiving Party and its related entities (e.g. contractors and subcontractors) only for the purposes of fulfilling the receiving Party's responsibilities under the B-BOP or SPICA Projects and that the identified and marked technical data shall not be disclosed or retransferred to any other entity without prior written permission of the document preparer.

	Observing Modes and Time Estimation	Ref.: Issue: Date: Page:	BBOP-DAP-RP-0002 0.5 23/06/2020 2/28
---	-------------------------------------	---	---

Document version tracking

Issue	Date	section	Description of Change
0.1	18/04/2019	n.a.	Began work on document
0.2	27/08/2019	7.3	Corrected mistakes in equations (incorrect use of notations) that lead to new optimal solution
		n.a.	Various corrections and improvement suggested by J. Delabrouille
0.3	14/10/2019	8	Initiated work on the sensitivity section
0.4	06/04/2020	8	Wrote section on the NEP and foregrounds. Included a description of the B-BOP pixels. Correct as well the consequence of a misunderstanding on the pixel absorbing area. Optical transmission applies to the source flux as well in flux limit equations.
0.5	23/06/2020	8	Added the Galactic ISM foreground and the definition of reference foreground cases. Updated the telescope emissivity.

The presented document is Proprietary information of the B-BOP Consortium. This document shall be used and disclosed by the receiving Party and its related entities (e.g. contractors and subcontractors) only for the purposes of fulfilling the receiving Party's responsibilities under the B-BOP or SPICA Projects and that the identified and marked technical data shall not be disclosed or retransferred to any other entity without prior written permission of the document preparer.



	Observing Modes and Time Estimation	Ref.: Issue: Date: Page:	BBOP-DAP-RP-0002 0.5 23/06/2020 3/28
--	-------------------------------------	---	---


Table of Contents

1	Purpose	4
2	Applicable & Reference Documents	5
	2.1 Applicable Documents	5
	2.2 Reference Documents	5
3	Acronyms	6
4	Introduction	7
5	Observing modes	7
6	General features and assumptions about B-BOP	8
7	On-source time, and optimisation of a scanning mode	9
	7.1 Definitions	10
	7.2 Defining the sky coverage	11
	7.3 Going to the map	13
8	Sensitivity	17
	8.1 The B-BOP pixels	17
	8.2 Deriving the <i>NEP</i>	19
	8.2.1 Flux contribution from a thermal source	19
	8.2.2 Noise equivalent power from a thermal source	21
	8.2.3 Application to the B-BOP pixels	22
	8.3 flux limits in total power	22
	8.3.1 Parameter definitions	22
	8.3.2 Estimation of the limiting flux	23
	8.3.3 The extended source case	23
	8.3.4 The point source case	24
	8.4 Flux limits in polarisation	24
	8.4.1 Parameter definitions	25
	8.4.2 Derivation of the signal-to-noise on absorbed power	25
	8.4.3 Estimation of the limiting flux	27
	8.4.4 The extended source case	28
	8.4.5 The point source case	28

	Observing Modes and Time Estimation	Ref.: Issue: Date: Page:	BBOP-DAP-RP-0002 0.5 23/06/2020 4/28
--	-------------------------------------	---	---

1 Purpose

This document aims at collecting information relative to the estimation of observing time with B-BOP, and therefore the instrument's sensitivity in various configurations. Since B-BOP is a mapping instrument, the document will start by covering possible observing modes that we may or may not implement. It will support the development of a time estimator for future observers, and contain justification for assumptions that will likely be buried inside the time estimator code. Starting at version 0.3, the equations derived here are implemented in a Python3 (currently 3.7.0) package (`timeEstimator3.py`) which has been used to compute a number of standard sensitivity numbers assembled in the B-BOP fact sheet v2.0.

	Observing Modes and Time Estimation	Ref.: Issue: Date: Page:	BBOP-DAP-RP-0002 0.5 23/06/2020 5/28
---	-------------------------------------	---	---


2 Applicable & Reference Documents

2.1 Applicable Documents

AD	Title	Reference	Date


2.2 Reference Documents

RD	Title	Reference	Date
RD1	Probing the cold magnetised Universe with B-BOP	PASA	2019
RD2	Compressed Sensing in Astronomy	IEEE journal of selected topics in signal processing	vol. 2 iss. 5 2008

	Observing Modes and Time Estimation	Ref.: Issue: Date: Page:	BBOP-DAP-RP-0002 0.5 23/06/2020 6/28
--	-------------------------------------	---	---

3 Acronyms

AOCS	Attitude and Orbit Control System
B-BOP	Magnetic Field (B) explorer with BOlometric Polarisers
LF	Low Frequency (as in low frequency noise)
NEP	Noise Equivalent Power (in $\text{W.Hz}^{-1/2}$)
PSF	Point Spread Function
TBC	To Be Checked/Confirmed

	Observing Modes and Time Estimation	Ref.: Issue: Date: Page:	BBOP-DAP-RP-0002 0.5 23/06/2020 7/28
--	-------------------------------------	---	---

4 Introduction

Estimating the time needed to perform an observation is the key element scientists want to be able to do when investigating whether a particular science program is do-able with a given instrument. And as there are quite a number of steps between the determination of the noise at detector level, and the sensitivity at the observation level, this is not an easy task. While ultimately we will publish tables of sensitivities, we need to collect in a stable, documented and maintained form the assumptions that we have made to go from what we have measured in the characterisation facilities to the sensitivity predictions in different observing modes.

While this document is being assembled, its section may appear in an order that may not be logical. It is expected that section re-ordering will occur as the document develops.

5 Observing modes


One important aspect of B-BOP as an instrument is to understand that it is designed to map areas significantly larger than its intrinsic field-of-view of $\sim 2.6'$. It will do so by scanning the sky along a rectangular grid in so-called “boustrophedon” mode as is shown on Figure 7.1. In this mode we use the spacecraft to perform long regular slews, called scan legs, in one direction, followed by a small step in the perpendicular direction. The length of a scan leg will typically range between some tens of arcminutes (e.g. when mapping individual objects and maximising the spatial coverage) to a few degrees (e.g. when mapping complete interstellar clouds or sections of the Galactic plane).

Another key point to keep in mind is that, since we are using bolometers, the principle of the measurement during the scan is that bolometers permanently adjust to the incoming flux, and the readout system samples their state (i.e. reads them) at a fixed frequency. There is no notion of integration, or integration time with the B-BOP detectors. For the sake of this document, one can consider that the operation of the detectors is completely independent from the choice of the observing mode parameters which only describe how the sky is going to be mapped.

The separation between two scan legs is made such that there is an overlap in the area covered by the back and forth scan legs. The amplitude of this overlap impacts the time needed to cover a given portion of the sky, as well as the sensitivity of the final map (see later). It is quite likely as well that the B-BOP bolometers will present a component of low-frequency (LF) noise which is generally handled by multiplying the number of times a given sky pixel is covered by detector pixels. This can either lead to decreasing the step between two scan legs (i.e. increasing the overlap region), or implementing a mode where the observation is done twice (or more) with different scan leg directions. For *Herschel*, both bolometer instruments (PACS & SPIRE) were systematically using two orthogonal scan directions per observations. As long as there exist no measurement on B-BOP detectors, we cannot quantify the LF noise component and therefore cannot tell whether we will place recommendations on these aspects of the observing mode parameters.

Still on the aspect of separation between scan legs, we mention here two extreme cases that will likely correspond to two implementations of the B-BOP observing mode:

- Maximising the separation (i.e. minimising the overlap) for science cases where the instantaneous sensitivity of B-BOP is sufficient and where the observer seeks to maximise the covered area per unit time.

	Observing Modes and Time Estimation	Ref.: Issue: Date: Page:	BBOP-DAP-RP-0002 0.5 23/06/2020 8/28
--	-------------------------------------	---	---

- Minimising the separation (i.e. maximising the overlap) when what is sought is the most homogenous sky coverage as possible, for instance if the observer intends to perform restoration of the spatial information “below” the pixel size.

A further parameter of the observing mode is the scanning speed, i.e. the speed at which the spacecraft is commanded to move along the scan leg. With detectors such as those of B-BOP, the allowed scan speeds are bracketed by two conditions. At the high end, we need to limit the scan speed because bolometers have a finite time constant (i.e. they adjust to a changing illumination in a finite time): when the scan speed is too high, the bolometer signal cannot adjust as fast as the illumination and we observe a blurring effect, or an increase of the point spread function (PSF) in the direction of the scan. This in turns increases the level of the confusion noise, which we want to avoid. At the low end, we are falling back on LF noise limitations: one way to consider this noise’s behaviour is as a drift of the signal level, independent of the illumination. The principles used to “filter” data from this noise component often rest on the assumption that the frequency domain in which LF noise dominates is different from that where the sky signal dominates, the latter being defined by the modulation frequency of the sky signal. In the scanning case, we modulate the signal by scanning and thus we must make sure that the scanning speed is large enough that for any pixel, modulation of its illumination (obtained by scanning the sky scene) is done at a higher frequency than the characteristic LF noise frequency.

Once again, in the absence of data on the detectors, it is not possible to determine what the recommended scan speed(s) should be. We simply recall here that with *Herschel*/PACS we offered 3 possibilities: 10, 20 and 60”/s. During calibration we did not notice any difference in data taken at 10 or 20”/s and thus almost all prime mode observations were done at 20”/s. In parallel mode we scanned at 60”/s (to follow a SPIRE constraint) and observed some degradation of the PSF. Therefore, for the sake of time estimation **we will base all our later computation on the assumption that SPICA is scanning at 20”/s during a B-BOP observation.**

To fully characterise an observation we need a few more parameters that do not strictly belong to the notion of observing mode, however we will mention them for completeness and because at least one of them play a role in the optimisation.


The first one is the orientation of the scan map on the sky, which is usually defined with the position angle of the scan leg direction (the angle with respect to the celestial north, measured eastward on a sky projection of the map), and the second is the orientation of the detector within the map, which we call the scanning angle and is measured in a spacecraft referential. It must be realised that these two parameters are not independent of one another due to the high pointing constraints of the SPICA spacecraft. In general the science fields of interest have no particular shape and thus there is no need to specify a preferred position angle on the sky.

All the parameters that define the observing mode are summarised in Table 5.1.

6 General features and assumptions about B-BOP

In this section we list a number of elements that we take for granted in this document, either because they are features of the instrument, or because they represent general and reasonable assumptions about its properties.

First the shape of the B-BOP instantaneous field of view is considered a square. This is absolutely true for Band 2 and 3 as they are made of a single 16×16, respectively 8×8 array,

	Observing Modes and Time Estimation	Ref.: BBOP-DAP-RP-0002 Issue: 0.5 Date: 23/06/2020 Page: 9/28	
--	-------------------------------------	--	--

Parameter	Notation	Probable range	Comment
Scan leg length	L_{leg}	10's of arcminutes to a few degrees	None
Separation between legs	Δ_{leg}	arcseconds to arcminutes	Capped by the array size
Scanning speed	v_{scan}	10-60''/s	Herschel range
Scanning angle	α	$[0, \pi/4]$	Angle between the scan direction and the detector axis
Position angle	θ	any	Position angle of a scan leg w.r.t. Celestial North

Table 5.1.: Parameters of the B-BOP observing mode. These define uniquely an observation, however it is likely that a subset only will be offered for selection to the observer (e.g. θ as it restricts the observability). Probable ranges are indicated to provide an idea of the values that need to be allowed by the AOCS. Instrumental properties will likely restrict these ranges.

this is less the case of Band 1 which is made of 4 16×16 arrays that are not tightly joined together. Nevertheless the 4 arrays are regularly placed inside a larger square. We will consider later the impact that the "blind" regions of the field of view in Band 1 have on the optimisation of the scan mode, and on the resulting sensitivity.


Then we achieve an instantaneous $0.6F\lambda$ sampling of the sky, i.e. there is no loss of spatial information due to the instantaneous sampling. This is absolutely true in total power (every pixels measures the total power it receives). This is less true in polarised intensity as the focal plan is a checker board of polarisation-sensitive pixels, alternating between two polarisation direction from one pixel to the next¹. In effect though, the sampling frequency is still the same although the sampling is now sparse rather than complete: we are missing flux but we are not losing information. As we are scanning, we know we will recover the missing flux, and extensive work on sparse sampling (also known as *compressed sensing*) shows that with a sparsity of $1/2$, we have more than enough information to restore the full signal (see for instance RD2).

7 On-source time, and optimisation of a scanning mode

Now that the observing mode of B-BOP is clarified and the basics of the instruments set, we will look into more details at the elements that constrain the parameters of the observing mode, and thus are needed to understand how observing times and sensitivities can be derived from the instantaneous performance of the detectors.

We warn that a reader with good intuition will likely find some of the following sections tedious (there is indeed little magic to be expected when scanning the sky with a square detector), however we wrote them so that even the obvious is supported by the appropriate, and hopefully rigorous, formalism.

¹In reality the polarisation sensitive element of the pixel does not directly measure the polarized intensity but for the sake of this document, we assume this representation is valid.

	Observing Modes and Time Estimation	Ref.: BBOP-DAP-RP-0002 Issue: 0.5 Date: 23/06/2020 Page: 10/28
--	-------------------------------------	---

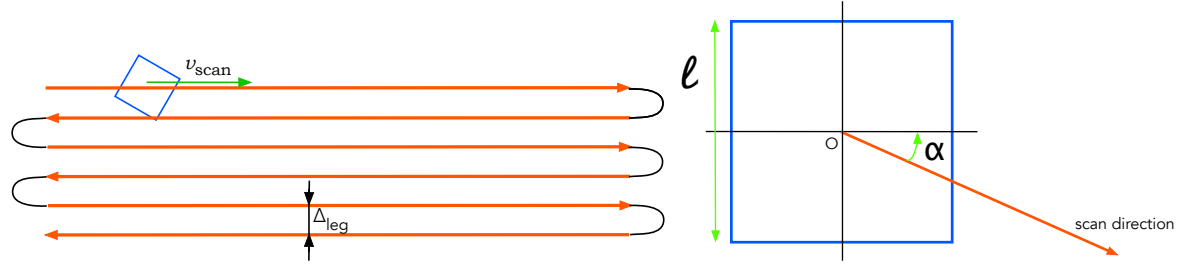


Figure 7.1.: Definition of basic parameters of the problem. On the left, the Boustrophedon scanning mode, where the telescope scans the sky in parallel lines, with curved trajectories in black to go from one line to the next. The angular separation between legs is noted Δ_{leg} . The blue square indicates an instantaneous position of the detector during the scan. On the right, the blue square represents again the array we are considering for the observation. The black lines are the reference axes for this array which is made of square pixels (these will be spacecraft axes eventually). The red arrow represents the scan direction and makes an angle α with respect to one of the main axis. Symmetry considerations show that $\alpha \in [0, \pi/4]$ covers all possible scanning strategies. We have also indicated the value of another parameter: l the array side length.

7.1 Definitions

One key number that we need to derive to get a sensitivity is the on-source time. With B-BOP which is a mapping instrument, this means computing the coverage factor, i.e. how many different detector samples see a given position of the sky during an observation. For a space instrument, there are not many possible choices to implement a mapping observing mode and as explained above, our working assumption is that SPICA will implement a “boustrophedon” mode (see Figure 7.1), where the sky is covered by back and forth scanning movements, each spaced by a certain angle.

This Figure illustrates the parameters of the observing mode (Table 5.1) that will play an important part in the optimisation, namely:

- α the angle between the scanning direction and one of the axes of the arrays. Because of intrinsic symmetries in the problem, $\alpha \in [0, \pi/4]$.
- Δ_{leg} the angular separation between two scan legs.
- v_{scan} the angular scan speed.

To these parameters we add the length of the array side, noted l . As mentioned before we do not consider here θ , the position angle of the scan leg, as it clearly does not allow any optimisation of the observing mode with respect to sensitivity in the map. For the same reason we do not consider L_{leg} , the scan leg length, as an optimisation parameter.

As a side note with future observers in mind, the parameters we have listed above, with the exception of l , define the list of parameters that an observer will have to set to define his/her observation. It is the purpose of this document to define within which range it is sensible to let the observer choose, with the implicit knowledge that to implement an observatory, it is better to leave as little choice to the observer as possible.



With these definitions of parameters, we can ask what is an optimal scanning mode? There are in fact quite a number of “dimensions” along which a scanning mode can be optimised. For instance, it can be optimised to recover a spatial sampling that has been lost through the use of pixels that are too large with respect to the telescope beam (e.g. the case of *Herschel*/SPIRE).

More relevant in our context is the efficiency of the mapping strategy, i.e. how much angular surface of the sky can be covered in a fixed amount of time. This will push for having Δ_{leg} as large as possible. However it is clear that a hard limit is reached when the angular separation is such that neighbouring scan legs no longer overlap. This will depend on the value of α . There is also a softer limit which comes from the instantaneous sky coverage, i.e. the amount of time that is spent on any given sky pixel of the map. It is clear that the smaller Δ_{leg} the larger this time (all parameters being kept equal), it is also clear the homogeneity of the sky coverage will also depend on Δ_{leg} and α .

Therefore one of the intermediate “variable” that we will need to define is how the sky coverage is related to the scanning parameters. By sky coverage we refer to the number of samples obtained on each sky pixel of the map. One can easily realise that for most choices of scanning parameters, the coverage will not be constant on the map, thus we are looking to quantify the distribution of sky coverage values generated by a given choice of scanning parameters.

7.2 Defining the sky coverage

The sky coverage here is the number of samples, or the amount of time spent per unit area of the sky, or sky pixel. We will not define it exactly but determine what it depends on. The left panel of Figure 7.2 shows how to derive this information: the maximum time that can be spent on a given sky pixel during a single scan leg is when the scan line that passes over this pixel has a maximum length when it crosses the array. And this maximum crossing length is always obtained for a line that crosses the array, through its center O , at the angle α . It is therefore straightforward to see that this length is:

$$l' = l / \cos \alpha, \quad (1)$$


which means that the maximum time spent on a given point in the sky along this scan leg is:

$$t_{\text{max}} = l' / (v_{\text{scan}} \cdot \cos \alpha). \quad (2)$$

Clearly only a strip of sky pixels will be observed for that duration: if we define b as the distance between a sky pixel and the line, passing through the centre O of the array along the scan direction, we can clearly see that as b increases there will come a value when the line drawn at this distance b from the scan direction passing through O no longer intercepts the array along the maximum path. This is illustrated on the right panel of Figure 7.2 which also highlights in pink the surface of the array that provides this maximum coverage for a single scan leg. Exploiting the symetries in the figure it is not too complicated to find the maximum value of b that still provides a maximum path through the detector, b_{m} , from the scanning parameters as:

$$b_{\text{m}} = \frac{l}{\sqrt{2}} \times \sin\left(\frac{\pi}{4} - \alpha\right). \quad (3)$$

Indeed, if we scan at 45° from the horizontal axis ($\pi/4$), $b_{\text{m}} = 0$ as indeed, only the diagonal

	Observing Modes and Time Estimation	Ref.: BBOP-DAP-RP-0002 Issue: 0.5 Date: 23/06/2020 Page: 12/28
--	-------------------------------------	---

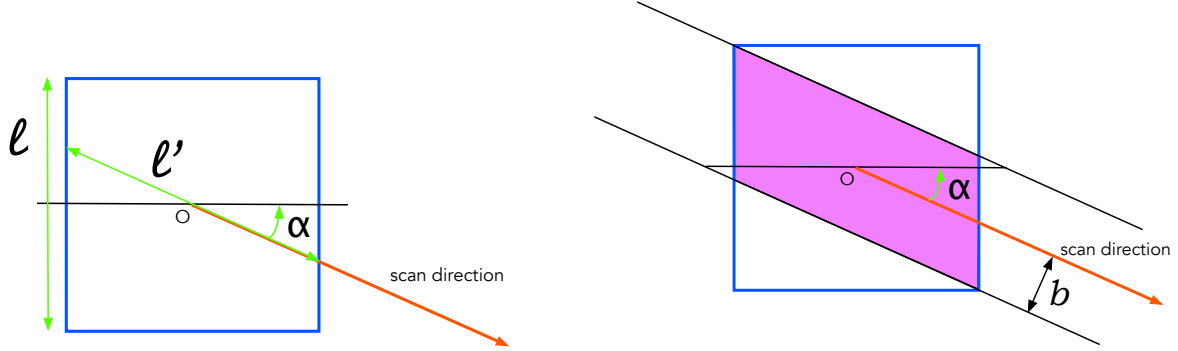


Figure 7.2.: *Left:* Definition of the maximum path length through the array. For a given scan direction, α , the maximum path length through the array is given by the line that crosses through the center of the array, O at an angle α with respect to the reference axis. *Right:* b is the maximum distance at which a sky pixel can be from the line that passes through O along the scan direction so that it still intercepts the maximum path on the array.

of the square realises the maximum path. If we scan along the horizontal axis² then $b_m = l/2$, i.e. the whole array realises the maximum path.

In that same line of thinking we can derive b_1 which is the “last” value of b for which a sky pixel is covered by that scan leg:

$$b_1 = \frac{l}{\sqrt{2}} \times \cos\left(\frac{\pi}{4} - \alpha\right). \quad (4)$$

Again to provide some sense of what this equation predicts let’s look at that same two cases: if we scan at 45° , we get that $b_1 = l/\sqrt{2}$, i.e. half the diagonal of our square detector, while if we scan at $\alpha = 0^\circ$, then $b_1 = l/2$. This, in fact, identifies $\alpha = 0^\circ$ as a special case where $b_m = b_1 = l/2$. In that case the computations we are going to make below is pointless: the length of the path on the array is constant and maximum. Optimizing that case is trivial, however, as we have said earlier, due to the presence of blind areas in B-BOP’s field of view aligned with the array axes, it is extremely unlikely that we would use a scanning angle of $\alpha = 0^\circ$. Thus in the remaining of this document we consider $\alpha \in]0, \pi/4]$

Finally, we can compute the length of the intercepted path on the detector for an “impact parameter” b between b_m and b_1 so that we will have all the elements we need to understand the coverage factor of a given scan map configuration. As this is a bit more complicated than the previous derivation, Figure 7.3 provides a geometric representation of the problem with the notations that we will use.

Using the figure, what we want to measure is the length $D'B'$, which we will note $l'(b)$.

First we note that we have two rectangular triangles in this figure, $D'AB'$ rectangular in A , and $B'EB$, rectangular in E , and that in these triangles we have $\widehat{D'B'A} = \widehat{BB'E} = \alpha$. Since BE

²given as a numerical application of the formula, as we will definitely not do that since in Band 1 it will leave blind areas in the map!

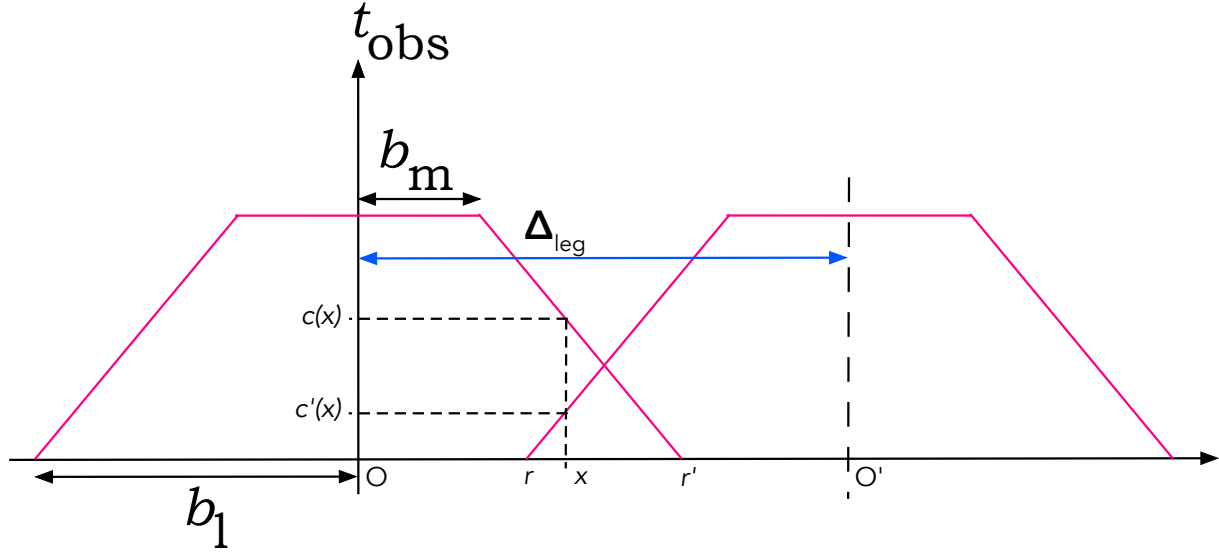


Figure 7.4.: A cut on the coverage factor along direction perpendicular to the scanning direction. We represent here the coverage function derived in equation 6 as a function of position across the scanning direction for two successive scan legs. Points labeled O and O' represent the location of the centre of the array as it crosses the cut line. We also report on this figure important dimensions that we will use in the text.

time only depends on the value of the impact parameter (i.e. the distance between a point in the sky and the trajectory of the center of the array on the sky), there is only one spatial dimension of the map we need to consider here: that perpendicular to the scan direction.

To clarify this and set the stage for this part of the document we show on Figure 7.4 the distribution of the observing time generated by two successive scan legs. On the first one, centered on O which represents the location of the array center as it crosses the line along which we have cut through the map, we have reported the two characteristic measures of the scan leg: b_m which is distance from O along which the observing time is maximum because we are crossing the longest path through the array, and b_1 which is the distance from O at which the array ceases to cover the sky. A second scan leg is represented, now centred on O' , and the distance OO' is the definition of the scan step, Δ_{leg} . The observing time produced by this configuration is the sum of the two red functions.

Looking at the effect of the parameter Δ_{leg} it is not too complicated to see that we can examine it on three different intervals:

- $\Delta_{\text{leg}} \in [0, 2 \times b_m]$ where the step is small enough that the top parts of the coverage overlap. This is typically a set-up where the aim is to achieve maximum sensitivity and possibly spatial sampling restoration, at the expense of a small total coverage.
- $\Delta_{\text{leg}} \in [2 \times b_m, b_m + b_1]$ where the step is now such that the coverage from the first leg starts decreasing before that from the second leg has reached its maximum, but where at maximum value of the scan step, coverage from the first leg decreases at the exact position



where coverage from the second leg increases.

- $\Delta_{\text{leg}} \in]b_m + b_1, 2 \times b_1]$ where the scan step still increases up to the point when the end of the coverage function of the first leg coincides with the beginning of the coverage of the second leg.

Using a scan step larger than $2 \times b_1$ does not make sense as it will create blind stripes in the map which will not be fully recovered by a second scan map using a different scanning direction.

Of course a scan map is made of more than 2 legs so in principle, the overlap can be generated by more than two legs. This happens when $\Delta_{\text{leg}} < b_1$, which, depending on the value of α occurs in the first or second interval described above³. In the present version of this document we are focusing on the main science case (mapping of the magnetic field in interstellar clouds), and thus we are aiming at an efficient coverage of large areas of the sky. We are thus not considering cases where more than 2 scan legs overlap, and in fact we are going to concentrate on the third case which likely contains a situation where the coverage is optimised with respect to uniformity and spatial efficiency.

Figure 7.4 is an illustration of a situation belonging to the third case. Along the abscissa we have noted r the location where the overlap begins, and r' the location where it ends. We have:

$$\begin{aligned} r &= \Delta_{\text{leg}} - b_1 \\ r' &= b_1. \end{aligned} \quad (7)$$

At the limits of the interval we are considering (third case above) we have, for the smallest value of the scan step, $r = b_m$ for an overlap length of $b_1 - b_m$, and, for the largest value of the scan step, $r = b_1$ and an overlap length reduced to 0.

Let us now consider a point x located within the overlap ($r \leq x \leq r'$), and call $c(x)$ the coverage at this location due to the first scan leg and $c'(x)$ the coverage at this location due to the second scan leg. We use for that the coverage formula of eq. (6) noting that for the first leg, x is identical to the impact parameter b , while for the second leg, the impact parameter corresponding to x is $\Delta_{\text{leg}} - x$. Thus we have:

$$\begin{aligned} c(x) &= \frac{1}{v_{\text{scan}} \times \cos \alpha} \times \left(l - \frac{x - b_m}{\sin \alpha} \right) \\ c'(x) &= \frac{1}{v_{\text{scan}} \times \cos \alpha} \times \left(l - \frac{\Delta_{\text{leg}} - x - b_m}{\sin \alpha} \right) \end{aligned} \quad (8)$$


The map coverage is the sum of these two functions and is:

$$C(x) = \frac{1}{v_{\text{scan}} \times \cos \alpha} \times \left(2 \times l - \frac{\Delta_{\text{leg}} - 2 \times b_m}{\sin \alpha} \right) \equiv C_{\text{over}} \quad (9)$$

While this is not completely unexpected from Figure 7.4, we see that in the overlap region between the scan, the coverage factor no longer depends on the position. Thus the generic pattern of the coverage in that interval is that it has two plateaus, one at $l/(v_{\text{scan}} \cos \alpha) \equiv C_{\text{max}}$ covered by the central part of the array and one at C_{over} , connected by regions of decreasing and increasing coverage if these two values are not identical.

Coming back to our original goal which is to optimise the coverage and the efficiency of the mapping mode, we can say that there are four conditions that should be made, the first two to define an homogenous map, and the last two to have an efficient mapping mode:

³From the expressions of b_m and b_1 one can show that this will occur in the first interval when $\alpha \leq 18.43^\circ$.

	Observing Modes and Time Estimation	Ref.: BBOP-DAP-RP-0002 Issue: 0.5 Date: 23/06/2020 Page: 16/28
---	--	---

1. There should not be transition region between the two coverage plateaus (at C_{\max} and C_{over}), which requires that $\Delta_{\text{leg}} = b_m + b_l$, i.e. we are at the beginning of the third interval defined above.
2. The two coverage plateaus should have the same level, i.e. $C_{\text{over}} = l/(v_{\text{scan}} \cos \alpha)$
3. We should cover the largest area in a given time, which means that for a given v_{scan} , Δ_{leg} should be maximum.
4. We should reach the highest coverage per sky position which means that C_{\max} should be maximum.

if we use condition #1 in equation (9), condition #2 becomes:

$$b_l - b_m = l \times \sin \alpha \quad (10)$$

b_l is defined in equation (4), b_m is defined in equation (3), where we can develop the cos and sin using trigonometric relations, remark that $\cos \pi/4 = \sin \pi/4 = 1/\sqrt{2}$ and realise that it is always true! Whatever the angle α , as long as $\Delta_{\text{leg}} = b_m + b_l$, we have optimal coverage.

However, developing the condition in #1 gives $\Delta_{\text{leg}} = l \times \cos \alpha$. Since $C_{\max} = l/(\cos \alpha \times v_{\text{scan}})$, showing quite clearly that for a given v_{scan} is it impossible to satisfy both conditions #3 and #4. Playing on v_{scan} does not allow to solve this dilemma as increasing it will indeed lead to a higher mapping efficiency (more area covered in a given total time), but will decrease the coverage per sky position. However while it is impossible to maximise both the coverage and the mapping efficiency, we can try and find an optimal compromise. A way to define this optimal compromise is to identify the value of α and that allow both the coverage and the mapping efficiency to reach the same fraction of their maximum value. Let's call f this fraction, we need to solve the system:


$$\begin{aligned} \Delta_{\text{leg}}(\alpha) = l \times \cos \alpha &= f \times \Delta_{\text{leg}}(\text{max}) = l \\ C_{\max}(\alpha) = \frac{l}{\cos \alpha \times v_{\text{scan}}} &= f \times C_{\max}(\text{max}) = \frac{\sqrt{2} \times l}{v_{\text{scan}}} \end{aligned} \quad (11)$$

From this system we easily obtain that the compromise is obtained for $\cos^2 \alpha = \sqrt{2}$ which numerically means a scanning angle of 32.8° where the coverage and mapping efficiency both reach 84% of their maximum value.

With this numerical value we can now define our optimal observing mode, in the sens of the mode that provides a map with uniform coverage, highest time per sky position and the most efficient use of observing time to cover the sky. This mode's parameter are listed in Table 7.1.

Practically, as B-BOP is a mapping instrument we will also need to now how these parameter translate into a mapping time (i.e. time to map a give sky area). Let's write done the equations that give that number for a 1 square degree area. The time to make a scan leg of 1° is simply $3600''/v_{\text{scan}}$ (as the scan speed is expressed in arcsecond per second) so we need to compute how many scan legs are required to produce a map whose width (direction perpendicular to the scan direction) is 1° . If we have N_{leg} scan legs, the width covered at C_{\max} is:

$$W = 2 \times b_m + (N_{\text{leg}} - 1) \times (b_m + b_l), \quad (12)$$

	Observing Modes and Time Estimation	Ref.: Issue: Date: Page:	BBOP-DAP-RP-0002 0.5 23/06/2020 17/28
---	-------------------------------------	---	--

Parameter Description	Value
Scan angle (α) w.r.t. detector	32.8°
Scan leg separation (Δ_{leg})	$l \times 0.84$
Observing time per sky point (t_{obs})	$l / (0.84 \times v_{\text{scan}})$
Time to map 1 square degree	$(3600'' / v_{\text{scan}}) \times [1.20 \times (3600'' / l + 0.54)]$

Table 7.1.: Summary of the parameters for the scanning mode that optimises the coverage homogeneity. In this table, l is expressed in arcseconds, and v_{scan} in arcsecond per second, thus both t_{obs} and the time to map 1 square degree are expressed in seconds.

which gives after some manipulations:

$$N_{\text{leg}} = \frac{1}{\cos \alpha} \times \left(\frac{W}{l} + \sin \alpha \right) \quad (13)$$

if we take $l = 160''$ and $v_{\text{scan}} = 20''/s$ (which are currently reasonable values for B-BOP) we get from the table that the observing time per sky point is 9.5 s, and that the time required to map a square degree is 1 h and 23 m.

8 Sensitivity

We now have a formula that relates the total observing time for a given area to the time spent per position in the map, which, for the time being, we will identify with the time spent sampling the brightness in a map pixel (equivalent to a detector pixel). Therefore we can now turn to the classical signal-to-noise equation to derive sensitivity numbers. This equation can be written as:


$$S/N = \frac{P_{\text{inc}}}{NEP_{\text{tot}}} \times \sqrt{2t_{\text{obs}}}. \quad (14)$$

Here P_{inc} is the incident power absorbed by the pixel, and NEP_{tot} is the total noise equivalent power of the detection system. S/N is the signal to noise of this measurement. However as the absorbed power is the sum of the power from the object of interest plus a wide range of contributions (astrophysical and instrumental, see below), this value of S/N is absolutely not the value that is of interest to the observer, and the task of this section will be to relate the expression of a “target” (s/n) in a referential that is familiar to an observer to the quantities present in eq. (14).

But there are a few things that we should do first. One is obviously deriving the noise equivalent power, but even more basically, we should introduce some features of our detectors that will provide some justification to the way we derived the applicable NEP and thus compute the sensitivity.

8.1 The B-BOP pixels

The detection method in B-BOP is rather innovative and as it has an impact on how we take into account the different sources of noise in our estimate of the sensitivity, it is worth spending some words on it. Instead of using polarised to filter the light along some polarisation direction

	Observing Modes and Time Estimation	Ref.: BBOP-DAP-RP-0002 Issue: 0.5 Date: 23/06/2020 Page: 18/28
---	-------------------------------------	---

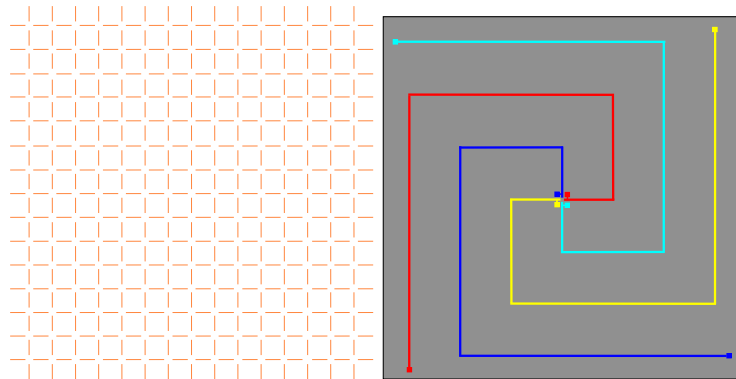



Figure 8.1.: left: the absorbing dipoles in the pixel. In each pixel we fill 100% of the pixel surface with absorbing dipoles with geometric parameters (length, width and spacings) adjusted to the central wavelength of the band. This adjustment is important to make the full surface of the pixel sensitive to the incoming radiation. Right: The thermally variable resistors that realise the bolometer part of the pixel. There are four such resistors, connected two by two (cyan with red, yellow with blue) by the readout circuit. Not shown in this picture are the load resistors, fixed resistors connected at the end of the bolometer resistors.

before it reaches the pixel, we have essentially implemented the polariser in the detection layer of the pixel. And we have combined that polariser with a bolometer to measure the absorbed power. In fact we implement two polarisers per pixel. This is going to be clearer on Fig. 8.1.

On the left of the figure we see the grid of dipoles that are placed inside the pixel. These dipoles will be used to create the polariser part of the pixel as the vertical, respectively horizontal, dipoles couple selectively to the radiation field according to the orientation and degree of the linearly polarized part. The dimension (length, width) and spacing of the dipoles are adjusted to the central wavelength of the band so as to make the entire surface of the pixel sensitive to radiation. Absorption efficiency is maximised by creating a resonating cavity below this absorbing grid (not shown on the figures). On the right we show the implementation of the thermally variable resistors in the pixels. The particular shape will become clear shortly. For the moment the important aspect is that these resistors will vary as a function of their temperature and that through a readout circuit (not shown) we will be able to make a measurement related to this temperature variation. Electrically, these resistors are placed in serie two by two (cyan with red and blue with yellow) and a fixed resistor is then connected to the end of each thermally variable resistor. This forms a Wheatstone bridge that we will not expand about here.

In order for this pixel to function we need to connect the absorbing polarisers to the thermally variable resistors, and this is done through a rather delicate structure that is built as the same time as the resistor, as shown in Fig. 8.2.

The challenge for these structures is to connect all the dipoles of a given orientation with two of the variable resistors, without touching the other two. To make this clear we have separated to two grids of dipoles. The left panel of Fig. 8.2 shows the connection of the horizontal dipoles with the red and yellow spirals. From the main bolometer spiral, branches are built to carry “sub-branches” where the dipoles are implanted. Exactly half of the dipoles are supported by each of the bolometer spirals. The central panel shows the same for the vertical dipoles. A careful observer will see that in fact the geometry of a spiral “arm” with all its branches and

	Observing Modes and Time Estimation	Ref.: BBOP-DAP-RP-0002 Issue: 0.5 Date: 23/06/2020 Page: 19/28
--	-------------------------------------	---

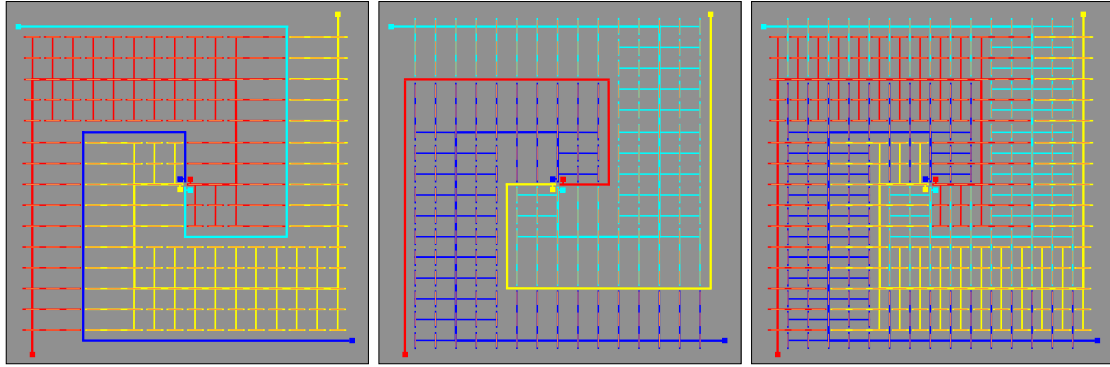


Figure 8.2.: Implementation of the structures that support the absorbing dipoles and connect selectively dipoles oriented in one direction with two of the variable resistors. For clarity we have separated the two orientations. On the left we see how the horizontally oriented dipoles are supported by structures connected to the red and yellow resistors, in the center we see how the vertically oriented dipoles are supported by structures connected to the cyan and blue resistors. On the right we see the complete pixel that shows how these structure manage to reside in the same pixel while avoiding each other.

sub-branches is rotated by 90° three times to produce the complete pixel structure (right-hand panel of the figure).

To summarise the particulars of our pixels we note that:

- 100% of the pixel surface is sensitive to radiation
- each polariser grid covers 100% of the pixel surface, i.e. the pixel solid angle per polariser is the same as for the total power.
- A pixel contains 4 thermally variable resistors, also called bolometers, but because of their geometry each bolometer “covers” $1/2$ of the pixel surface, not $1/4^{th}$.


8.2 Deriving the *NEP*

In this section we are going to derive the equations needed to compute the noise equivalent power (*NEP*) that should enter eq (14). We are going to make one strong assumption which is that all *NEP* contributions, except that from the detector itself, can be approximated as coming from a thermal component. This is very close to be true for all the elements such as the telescope mirrors and the instrument optics. This is true for the Cosmic Microwave Component (CMB), but it is less so for the zodiacal emission, the Cosmic Infrared Background (CIB) or the Galactic Interstellar emission (ISM).

Concerning the ISM component, as it is the main science target of a large fraction of the programs, it remains debatable whether its contribution to the *NEP* that enters the sensitivity estimation is mandated for all science cases.

8.2.1 Flux contribution from a thermal source

Let’s use this section to set some notation, and compute some estimates of the background flux under which B-BOP’s detector will operate. A thermal source will be characterised by a

	Observing Modes and Time Estimation	Ref.: Issue: Date: Page:	BBOP-DAP-RP-0002 0.5 23/06/2020 20/28
---	--	---	--

temperature, T , and an emissivity, $\epsilon(\nu)$, where we account for the fact that the emissivity may have a spectral dependency. In that case the power that this source will contribute in a pixel of our detector is proportional to:

$$P_{\text{th}}(\nu) \propto \epsilon(\nu) 2 \frac{h\nu^3}{c^2} \frac{1}{e^{h\nu/kT} - 1} \quad (15)$$

Where the factor of 2 in front can be seen as coming from the classical representation of unpolarised light as the superposition of two orthogonal linearly polarised waves (this will become relevant later on). The proportionality sign can be turned into an equal sign by taking into account the area of the emitting source, A_{src} , the solid angle of our pixel, ω_{pix} , the transmission of the instrument between the thermal source and the detector, t_{opt} . Finally, since we are using an instrument with broad bands, the value that matters is integrated over the filter transmission, $T(\nu)$, to give:


$$P_{\text{th}} = A_{\text{src}} \omega_{\text{pix}} t_{\text{opt}} \int_{\nu} T(\nu) \epsilon(\nu) 2 \frac{h\nu^3}{c^2} \frac{1}{e^{h\nu/kT} - 1} d\nu \quad (16)$$

This gives the background power that pixels sensitive to the total power of the incoming light will receive from a thermal source. Our pixels however function simultaneously in two modes, one where they are sensitive to the total power, and one where they are sensitive to the balance between two orthogonal polarisations. Depending on the case we consider, the relevant background contribution is given by eq. (16) in case of total power mode, or half of it in case of polarisation mode. This is because, as we have shown above independent of the mode we are working in, the effective pixel solid angle is still the same.

As mentioned in the beginning of this section, we consider as contributing to the background the following elements (moving outward from the detector):

- The optical elements (mirrors and dichroic mirrors) within the camera optics at 1.8 K. In the time estimator we consider that there are on average 5 optical surfaces on the path to each band. We also attribute to each of them an emissivity of 3%, and consider that the optical transmission is globally 0.5.
- The mirrors in the entrance optics at 4.8 K. Similarly in the time estimator we consider that there are 7 optical surfaces in this entrance optics, and we use the same emissivity and optical transmission as above.
- The telescope mirrors (M1 and M2) at 8.0 K. In the time estimator we consider that there are two optical surfaces with emissivity $\epsilon(\lambda) = 0.01308 \times \lambda_{\mu\text{m}}^{-1/2} + 0.3276 \times \lambda_{\mu\text{m}}^{-1}$ each. The optical transmission is also 0.5.
- The zodiacal light represented in our bands by a 265 K black-body with an emissivity of 10^{-7} .
- The Galactic ISM represented in our bands by at 20.7 K modified black-body, with an emissivity scaling as $\lambda^{-1.5}$ (these numbers were derived from a fit to the output of the Euclid foreground model⁴).
- The Cosmic Infrared Background (unresolved galaxies) represented in our bands by a 30 K black-body with an emissivity of 2.25×10^{-6} .
- The Cosmological Microwave Background as a perfect 2.725 K black-body.

⁴available at <https://irsa.ipac.caltech.edu/applications/BackgroundModel/>

	Observing Modes and Time Estimation	Ref.: BBOP-DAP-RP-0002 Issue: 0.5 Date: 23/06/2020 Page: 21/28
---	-------------------------------------	---

Note that most of the parameters above are assumptions/allocations made to build the time estimator code. As of this version very few of them rest on actual measurements or rigorous apportionments. This will obviously change as the instrument matures.

Finally, in the implementation of the time estimator, to reflect the fact that the astrophysical components of the background vary spatially, we have defined a 5 different scalings corresponding to typical regions in the Ecliptic, a high ecliptic latitude field for extragalactic studies, two position in the Galactic plane with high or low ISM contribution, and finally a reference one which uses the numerical values above but cancels the ISM component (mostly to allow comparisons with past sensitivity estimates that did not incorporate that component).

8.2.2 Noise equivalent power from a thermal source

We recall here the general equations to compute this component and will then see how this applies in practice to the thermal sources we have identified above.

For a black-body source characterised by its temperature T the *r.m.s.* of the number of photons of frequency ν emitted per unit time is given by:

$$[r.m.s.(N(\nu))]^2 = \frac{1}{e^{h\nu/kT} - 1} \times \left(\frac{1}{e^{h\nu/kT} - 1} + 1 \right). \quad (17)$$

The term $1/(e^{h\nu/kT} - 1)$ is called the photon occupation number and is linked to the stochastic nature of the emission and the particular spectrum of the black-body. In our case, we are not observing perfect black-bodies but rather sources that have a given emissivity, $\epsilon(\nu)$, and we observe them with a system that has a given transmission. Both of these correspond to stochastic processes and affect the photon occupation number and thus modify eq. (17) so that is should be written:


$$[r.m.s.(N(\nu))]^2 = \frac{\epsilon(\nu)t_{\text{opt}}t_{\text{filt}}(\nu)}{e^{h\nu/kT} - 1} \times \left(\frac{\epsilon(\nu)t_{\text{opt}}t_{\text{filt}}(\nu)}{e^{h\nu/kT} - 1} + 1 \right). \quad (18)$$

In eq. (18) we have separated the transmission into a part linked to the optical system, which we consider independent of the frequency, and a part linked to the filter system, for which the frequency dependence cannot be neglected.

To go from this formula, which is dimensionless, to the *NEP*, that is generally expressed in $\text{W}\cdot\text{Hz}^{-1/2}$ we will need to apply a certain number of factors to it. The first is the energy, $h\nu$ of the photon, the second is a weight of each frequency in the emitted spectrum, $h\nu^3/c^2$, then we have to take into account the beam étendue under which we are viewing this source, $A_{\text{tel}}\omega_{\text{pix}}$, i.e. the telescope area multiplied by the pixel solid angle. And then as we want to express the noise in a bandwidth of 1 Hz, we have a factor of 2 as well. These factors do not correspond to stochastic processes and therefore do not enter the photon occupation number but rather just scale the *r.m.s.*:

$$NEP_{\text{therm}}^2 = \int_{\nu} 2A_{\text{tel}}\omega_{\text{pix}}(h\nu) \frac{h\nu^3}{c^2} \frac{\epsilon(\nu)t_{\text{opt}}t_{\text{filt}}(\nu)}{e^{h\nu/kT} - 1} \times \left(\frac{\epsilon(\nu)t_{\text{opt}}t_{\text{filt}}(\nu)}{e^{h\nu/kT} - 1} + 1 \right) d\nu. \quad (19)$$

As mentioned above this is the *NEP* associated to one of the two linearly polarised states that photons can have in this thermal emission and depending of whether or not the detection system is sensitive to polarisation, another factor of 2 must be introduced to account for the full thermal *NEP*.

	Observing Modes and Time Estimation	Ref.: BBOP-DAP-RP-0002 Issue: 0.5 Date: 23/06/2020 Page: 22/28
---	-------------------------------------	---

8.2.3 Application to the B-BOP pixels

In our case, as we have explained in section 8.1, our detectors are intrinsically selective to polarisation therefore when considering the background NEP that one bolometer branch will be sensitive to, eq. (19) is the equation to consider. There is one small catch to consider and this is that for one bolometer branch (of which there are 4 in the pixel) the effective solid angle to consider is not ω_{pix} , the solid angle of the full pixel, but $\omega_{\text{pix}}/2$, thus the thermal NEP collected by one spiral arm of our detector is expressed as:

$$NEP_{\text{therm,B-BOP}}^2 = \int_{\nu} A_{\text{tel}} \omega_{\text{pix}} (h\nu) \frac{h\nu^3}{c^2} \frac{\epsilon(\nu) t_{\text{opt}} t_{\text{filt}}(\nu)}{e^{h\nu/kT} - 1} \times \left(\frac{\epsilon(\nu) t_{\text{opt}} t_{\text{filt}}(\nu)}{e^{h\nu/kT} - 1} + 1 \right) d\nu. \quad (20)$$

Finally as all the measurements that we perform combine all 4 bolometers (additively or differentially depending on whether one performs a total power or polarisation measurement), for our sensitivity computation the total NEP to consider is:

$$NEP_{\text{tot}} = \sqrt{NEP_{\text{det}}^2 + 4 \times \sum_{\text{src}} NEP_{\text{therm}}^2}, \quad (21)$$

where the summation under the square root is over the thermal sources that are present in the field of view and filling the beam and NEP_{det} is the detector contribution, the element on which the polarisation requirements will place performance requirements.


8.3 flux limits in total power

When the observer is interested in the total power of the source of interest, even though we have quite particular pixels, the input parameters for the sensitivity derivation are quite simple.

8.3.1 Parameter definitions

Clearly the first input parameter provided by the observer is the signal-to-noise on the target, (s/n) . We are using a different notation from eq. (14) because this is indeed a very different quantity: in particular it is in general the signal-to-noise measured after photometry has been performed on the target of interest. In the extended source case, this means subtracting a background value, and in the point source case this means integrating within an aperture and subtracting a background. The impact of these operations on the signal-to-noise recorded at the pixel level must be taken into account.

The second important parameter is the on-source time. In the case of a total power measurement, all pixels are the same therefore the on-source time to consider for the sensitivity equation is directly that given by the observing mode, t_{obs} . In polarisation mode, we need to acknowledge the fact that we have two types of pixels, and that it is the combination of these two sets of measurements that will yield the polarisation observation. As each type fills half the field of view, the effective on-source time it in that case $t_{\text{obs}}/2$. We will take that into account in Section 8.4.

	Observing Modes and Time Estimation	Ref.: BBOP-DAP-RP-0002 Issue: 0.5 Date: 23/06/2020 Page: 23/28
---	-------------------------------------	---

8.3.2 Estimation of the limiting flux

Eq. (14) defines the relation between the signal to noise in the pixel, the incident power absorbed by the pixel, the noise equivalent power and the observing time, but as $S/N = P_{\text{inc}}/\sigma_{\text{inc}}$ by definition, we can also use it to define the noise level associated to the measurement:

$$\sigma_{\text{inc}} = \frac{NEP_{\text{tot}}}{\sqrt{2t_{\text{obs}}}} \quad (22)$$

Noting P_s the source power that is absorbed by the pixel⁵, we can state that the signal-to-noise ratio relevant for the source signal per pixel is P_s/σ_{inc} , thus provided we can derive from the user provided (s/n) a prescription for this source signal-to-noise level per pixel, we can derive the limiting source power that will allow such detection.

Let's work out now how we specify the signal-to-noise to be reached at the pixel level from the user input. For that we will have to treat the extended and point source cases separately.

8.3.3 The extended source case

When the target is an extended source, we need to compute a surface brightness limit. This is rather straightforward from the expressions we have been using as a flux per pixel is already a surface brightness unit and we will only need to divide by ω_{pix}^i , the solid angle of the pixel in band i to obtain quantities in units familiar to an observer.

The one aspect to treat carefully the relation between the user-provided signal-to-noise ratio and that which is measured at the pixel level by P_s/σ_{inc} . As we mentioned in the beginning we consider that the user provides a signal-to-noise ratio (s/n) that refers to a post-photometric measurement state of the data, which, in the extended source case means a background subtraction. As noise contributes both to the background determination and to the source determination, this means that the signal to noise at the pixel level has to be $\sqrt{2}$ higher⁶, i.e. we can write that:

$$\frac{P_s}{\sigma_{\text{inc}}} = (s/n)\sqrt{2}, \quad (23)$$


To convert a power absorbed by a pixel into a spectral density illuminating that pixel we have to apply some correcting factors. First we have to divide it by the filter bandpass $\Delta\nu_i$ to get a spectral density (i refers to the B-BOP band, 1, 2, or 3). This can be obtained from the filter profile and a spectral convention, which we take as $f_\nu \propto \nu^{-1}$. Then we have to divide by the collecting surface A_{tel} to get a flux⁷. Finally we have to remember that only a fraction t_{opt} of the source flux at the telescope aperture reaches the detector pixel. Therefore the relation between the source flux illuminating the pixel (in $\text{W.m}^{-2}.\text{Hz}^{-1}$) and the power it contributes to the power absorbed in that pixel (in W) is:

$$f_\nu^i = \frac{P_s}{A_{\text{tel}} \Delta\nu_i t_{\text{opt}}}, \quad (24)$$

⁵ $P_{\text{inc}} = P_s + P_b$, the incident power absorbed results from a contribution by the source of interest and by the background.

⁶This can be considered an upper limit as the background level is usually determined with much more than one pixel measurement, however this whole sensitivity document tries to be on the safe side, hence this factor.

⁷At this stage we incorrectly mentioned in preview versions of this report that one also had to correct for the fact that only 1/2 of the incident power could be absorbed by a pixel due to the specific implementation of the dipole grids. As explained in Section 8.1 this is not true, all the incident power can be absorbed.

	Observing Modes and Time Estimation	Ref.: BBOP-DAP-RP-0002 Issue: 0.5 Date: 23/06/2020 Page: 24/28
---	-------------------------------------	---

where we acknowledge that this assumes that 100% of the flux illuminating the pixel is absorbed, a fact that is close to be true with B-BOP pixels.

Therefore, combining all these factors and expressions, we obtain:

$$f_{\nu,es}^i = \frac{1}{A_{\text{tel}} \omega_{\text{pix}}^i \Delta\nu_i t_{\text{opt}}} (s/n) \frac{NEP_{\text{tot}}}{\sqrt{t_{\text{obs}}}}, \quad (25)$$

where the flux limit is expressed in $\text{W.m}^{-2}.\text{Hz}^{-1}.\text{sr}^{-1}$ and (s/n) is the signal-to-noise value provided by the user.

8.3.4 The point source case

We now need to compute a flux limit which corresponds to the total source flux, which is the value on which the user-provided (s/n) applies. We need to be a little bit more careful. We will assume that point source photometry is performed using aperture photometry, with an aperture that covers N_{aper} pixels, and that within this aperture, the source power is uniformly distributed. Photometry is performed by summing the flux measured in the pixels, which means that we can relax the pixel signal-to-noise ratio by a factor $1/\sqrt{N_{\text{aper}}}$, i.e. we can have $P_s/\sigma_{\text{inc}} = (s/n)/\sqrt{N_{\text{aper}}}$. This is not all as photometry also means background subtraction and therefore the relation at the pixel level is really:

$$\frac{P_s}{\sigma_{\text{inc}}} = (s/n) \sqrt{\frac{2}{N_{\text{aper}}}} \quad (26)$$

Now from this source power per pixel we obtain the source power by a number of transformations. First we multiply it by the number of pixels in the aperture, N_{aper} . Then we take into account the fact that only a fraction of the total point source power is within this aperture (this is the definition of the Encircled Energy Fraction) so we need to divide by EEF_{aper} , the fraction of total power in the aperture. Dividing by the bandpass $\Delta\nu_i$, the collecting area A_{tel} , and the optical transmission finally transforms that limiting power into the limiting point source flux:


$$f_{\nu,ps}^i = \frac{1}{A_{\text{tel}} \Delta\nu_i t_{\text{opt}}} \frac{\sqrt{N_{\text{aper}}}}{EEF_{\text{aper}}} (s/n) \frac{NEP_{\text{tot}}}{\sqrt{t_{\text{obs}}}}, \quad (27)$$

where the flux limit is expressed in $\text{W.m}^{-2}.\text{Hz}^{-1}$ and (s/n) is the signal-to-noise value provided by the user.

8.4 Flux limits in polarisation

Note: This section contains a set of equations developed to derive sensitivities for the polarimetric mode of B-BOP. The equations themselves should be mathematically correct (at least we have taken great care of this) and as consistent as possible with those derived in the total power mode. However they are developed following a measurement concept that is not strictly that of the B-BOP detectors and therefore the sensitivities that we derive here should be considered preliminary.

When the observer is interested in deriving polarisation parameters (e.g. polarisation fraction and angle, or stokes parameter Q and U) the meaning of some input parameters changes, and we also have to take into account the particulars of our detector pixels.

	Observing Modes and Time Estimation	Ref.: Issue: Date: Page:	BBOP-DAP-RP-0002 0.5 23/06/2020 25/28
---	-------------------------------------	---	--

8.4.1 Parameter definitions

In a polarisation measurement, we consider that the observer is after the measurement of the fraction of the source power that is linearly polarised, p and the orientation of this linear polarisation as a function of position. We will address the question of angle in future versions of this report. When expressing the observation target, the user will provide an expected polarisation fraction p and a signal-to-noise ratio $(s/n)_p$. Contrary to the total power case where this signal-to-noise ratio applies on the source power, here it applies to the polarisation fraction so that we must consider that:

$$(s/n)_p = p/\sigma_p \quad (28)$$

is the signal-to-noise provided by the user (the p in subscript is meant to differentiate that signal-to-noise from the total power case and signifies that it applies to the polarisation fraction measurement). We will see how this can be related to the signal-to-noise that must be obtained on the measured power.

A second parameter necessary in the sensitivity estimation is the time spend on any given point of the map, the “on-source” time. As amply addressed in section 7, the observing mode will allow to derive that time from the area that the user wants to map. However in the case of a measurement targeting polarisation parameters, we must remember that we have in each array two kinds of pixels, each measuring how the incoming power is absorbed by two sets of dipoles, oriented at 90° of each other inside a single pixel, and rotated by 45° from one pixel to the next. The derivation of the polarisation parameters requires a measurement of the same point in the sky by both kinds of pixels. This means that the effective on-source time for polarisation measurement per pixel type is $1/2$ of the total on-source time derived from the observing mode:

$$t_{\text{obs}}^p = t_{\text{obs}}/2 \quad (29)$$


Third, we need to consider how the particular features of the pixel impact the *NEP* contributors: each pixel consists of 4 grid of absorbing dipoles, each covering $1/2^{\text{th}}$ of the pixel surface⁸, and each containing dipoles oriented in a single direction. Thus when considering dipoles oriented in a given direction, they can absorb at most $1/2$ of the total power they intercept but they do this on the full solid angle of the pixel (their filling factor).

8.4.2 Derivation of the signal-to-noise on absorbed power

To be able to use eq. (14) to derive the sensitivity limit in the point or extended source case, we must first relate $(s/n)_p$ to the required signal to noise in the detection system. As mentioned many times we absorb the incoming power with grids of dipoles oriented at 0° , 90° , 45° , and -45° , and we derive the polarisation parameters of the incoming light be comparing the power measured by each of these grid. We shall use the notations P^0 , P^{90} , P^{45} , and P^{-45} to refer to the power absorbed by each of these grid. Because of these orientations one can also use the capital letters L and V to refer to each type of pixel. In the following equations, when the superscripts disappear in the notation, this means that we have summed the power absorbed by the two grids inside the pixel (total power mode).

Furthermore we consider that the power falling on the pixels consists of the power of the source of interest, linearly polarised at some level p , and the power from the backgrounds,

⁸if that is still mystifying you, go back to Section 8.1 and remember that it mystified the author of this report as well.

	Observing Modes and Time Estimation	Ref.: BBOP-DAP-RP-0002 Issue: 0.5 Date: 23/06/2020 Page: 26/28
---	-------------------------------------	---

which we consider unpolarised, that combines both the astrophysical background in the scene we observe and the thermal backgrounds produced by telescope and other components. To distinguish between the two we shall use the notations P_s and P_b , and note P_t the sum of the two.

In practice, the polarisation parameters will be derived from the measurement of the imbalance between the power absorbed in two perpendicular dipole grids, by using this absorbed power to modify thermally variable resistors inside a Wheatstone bridge. Thus we are not measuring the powers on the different dipole grids, but for the sake of this sensitivity derivation we will assume that we have a method to recover that information.

Let's now define the ratio r of these absorbed powers:

$$\begin{aligned} r_L &= \frac{P_t^0 - P_t^{90}}{P_t^0 + P_t^{90}} \\ r_V &= \frac{P_t^{45} - P_t^{-45}}{P_t^{45} + P_t^{-45}} \end{aligned} \quad (30)$$

Let's develop one of these ratios (the arithmetics are the same). As we assume that only the source component is polarised, the imbalance between the two measurements made with orthogonal dipoles is only due to the source. So:

$$r_L = \frac{P_s^0 - P_s^{90}}{P_t} = \frac{P_s^0 - P_s^{90}}{P_s} \times \frac{P_s}{P_t}. \quad (31)$$

and then we will make the “wild” assumption that:

$$p = \frac{P_s^0 - P_s^{90}}{P_s} \quad (32)$$


This is a strong assumption because it implies that the direction of linear polarisation is aligned with one of the dipole network. However, given that we have dipoles oriented along any multiple of 45° , this may not be as incorrect as one could think of (the maximum error we are making on p is probably of the order of 30%, i.e. $1 - \cos \pi/4$).

Thus we can write that:

$$p = r_L \times \frac{P_t}{P_s} = \frac{P_t^0 - P_t^{90}}{P_s}. \quad (33)$$

From this equation we are going to derive one that links the user provided $(s/n)_p$ to quantities that are measured in our device. Let's note σ^P (note the P is an exponent here) the r.m.s. of the fluctuations of any of the polarisation component of the incoming power (P_t^0 , P_t^{90} , P_t^{45} , or P_t^{-45}). Because we are considering cases where the polarisation fraction is low we can assume that this r.m.s. is the same for any of these components. We can use error propagation relations to derive from eq. (33) the relation between the different error amplitudes of each factor in the equation:

$$\frac{\sigma_p}{p} = \sqrt{\left(\frac{\sigma^{(P_t^0 - P_t^{90})}}{P_t^0 - P_t^{90}}\right)^2 + \left(\frac{\sigma^{P_s}}{P_s}\right)^2}. \quad (34)$$

	Observing Modes and Time Estimation	Ref.: BBOP-DAP-RP-0002 Issue: 0.5 Date: 23/06/2020 Page: 27/28
---	--	---

The r.m.s. of the quantity $(P_t^0 - P_t^{90})$ is $\sqrt{2}\sigma^P$, and as $P_s = P_t - P_b$, and $P_t = P_t^0 + P_t^{90}$, we can write that $\sigma^{P_s} = \sqrt{2}\sigma^{P_t} = 2\sigma^P$. Therefore we can rewrite the equation above as:

$$\frac{\sigma_p}{p} = \sqrt{\frac{2(\sigma^P)^2}{(P_t^0 - P_t^{90})^2} + \frac{4(\sigma^P)^2}{P_s^2}} = \sqrt{2} \frac{\sigma^P}{P_s} \sqrt{2 + \frac{P_s^2}{(P_t^0 - P_t^{90})^2}}. \quad (35)$$

As $P_t^0 - P_t^{90} = P_s^0 - P_s^{90}$ since only the source component is polarised by assumption, the last ratio is in fact $1/p^2$ and thus we have (identifying appropriately the user provided signal-to-noise ratio σ_p/p):

$$P_s = \sqrt{2}(s/n)_p \sigma^P \sqrt{2 + \frac{1}{p^2}} \quad (36)$$

We see from this equation that for a given observation (that defines σ^P as we will see in a moment), the polarisation fraction impacts the flux limit: the lower the polarisation fraction and the higher the flux limit for a given requested signal to noise on the polarisation fraction (which is expected). The presence of the number 2 in the square root next to the polarisation fraction translates the fact that we have an equation on the source power, which results from a subtraction of the background power.

8.4.3 Estimation of the limiting flux

We now need to express σ^P and for this we go back to eq. (14). It writes:

$$S/N = \frac{P_{\text{inc}}}{NEP_{\text{tot}}} \times \sqrt{2t_{\text{obs}}}. \quad (37)$$

In our particular case, S/N is by definition P_t^i/σ^P , with the superscript i is for 0, 90, 45, and -45, P_{inc} is in fact P_t^i , and t_{obs} is t_{obs}^p , half of the total on-source time predicted by the observing mode and observed area. Therefore we can write:

$$\sigma^P = \frac{NEP_{\text{tot}}}{\sqrt{2t_{\text{obs}}^p}}, \quad (38)$$


So that now we can write the limiting flux equation completely with known quantities as:

$$P_s = \sqrt{2}(s/n)_p NEP_{\text{tot}} \frac{1}{\sqrt{t_{\text{obs}}}} \sqrt{2 + \frac{1}{p^2}}, \quad (39)$$

where P_s is the total power from the source falling on the pixel.

There however still are operations to perform to transform this power P_s into the flux limit that can be provided to the observer.

First this is the power from the source that reaches the pixel, so we need to divide it by the optical transmission t_{opt} of the system to recover the power at the telescope aperture. Then what we are deriving is a power (in W), and we need to provide the user with a spectral flux density ($\text{W.m}^{-2}.\text{Hz}^{-1}$) or surface brightness ($\text{W.m}^{-2}.\text{Hz}^{-1}.\text{sr}^{-1}$). To convert to a flux we will divide by the collecting surface of the telescope (A_{tel}), to convert to spectral density we will divide by a bandpass $\Delta\nu_i$ taken from the filter profiles, assuming a spectral convention $f_\nu \propto \nu^{-1}$ as is classical for this spectral domain, where i is 1, 2 or 3 to refer to the B-BOP bandpasses.

	Observing Modes and Time Estimation	Ref.: BBOP-DAP-RP-0002 Issue: 0.5 Date: 23/06/2020 Page: 28/28
---	--	---

The conversion to a surface brightness or a flux density in fact reflects the division of sensitivity quotation in two cases, that of a point source and that of an extended source. We will treat them separately. Note that in both case in the following we make no further “correction” for the fact that a photometric measurement requires a background subtraction as in the above derivation we have obtained a relation between measured quantities and the background-subtracted source quantity.

8.4.4 The extended source case

This is the simplest case as by using the pixel solid angle ω_{pix}^i we can directly convert P_s into a surface brightness. Thus the surface brightness flux limit f_{ν}^i can be written as:

$$f_{\nu,es}^i = \frac{1}{A_{\text{tel}} \omega_{\text{pix}}^i \Delta\nu_i t_{\text{opt}}} \sqrt{2} (s/n)_p \text{NEP}_{\text{tot}} \frac{1}{\sqrt{t_{\text{obs}}}} \sqrt{2 + \frac{1}{p^2}}, \quad (40)$$

where the flux limit is expressed in $\text{W.m}^{-2}.\text{Hz}^{-1}.\text{sr}^{-1}$, $(s/n)_p$ is the signal-to-noise value provided by the user, that applies to the polarisation fraction p also provided by the user.

8.4.5 The point source case

For this case we have to be a bit more careful: the flux of a point source does not fall into a single pixel, therefore P_s derived above needs some manipulation before we can relate it to the flux of a point source. In general, a point source measurement is the result of an integration into an aperture of a given size, followed by a correction for the flux that falls beyond that aperture. Considering this, we can assume that when the observer states that he/she wants to reach a certain $(s/n)_p$ on the polarised fraction of the flux of a point source, this applies after the aperture photometry has been performed).

Therefore we will assume that if the aperture consists of N_{aper} pixels, (a) the flux is distributed homogeneously in them, and (b) the (s/n) to be reached on the polarisation fraction per pixel is relaxed by $1/\sqrt{N_{\text{aper}}}$. Therefore eq. (39) becomes:

$$P_s = \sqrt{2} \frac{1}{\sqrt{N_{\text{aper}}}} (s/n)_p \text{NEP}_{\text{tot}} \frac{1}{\sqrt{t_{\text{obs}}}} \sqrt{2 + \frac{1}{p^2}} \quad (41)$$

This is the power absorbed by one pixel. Then we need to multiply this by N_{aper} to get the power inside the aperture, and then divide by the Encircled Energy Fraction, EEF_{aper} the fraction of the point source flux falling inside the aperture, to get the point source power. Dividing by $\Delta\nu^i$ and A_{tel} and t_{opt} will give us the limiting point source spectral flux density:

$$f_{\nu,ps}^i = \frac{1}{A_{\text{tel}} \Delta\nu_i t_{\text{opt}}} \sqrt{2} \frac{\sqrt{N_{\text{aper}}}}{EEF_{\text{aper}}} (s/n)_p \text{NEP}_{\text{tot}} \frac{1}{\sqrt{t_{\text{obs}}}} \sqrt{2 + \frac{1}{p^2}}, \quad (42)$$

where the flux limit is expressed in $\text{W.m}^{-2}.\text{Hz}^{-1}$, $(s/n)_p$ is the signal-to-noise value provided by the user, that applies to the polarisation fraction p also provided by the user.